Continental Shelf Circulation Induced by a Moving, Localized Wind Stress

JOHN M. KLINCK,[1] LEONARD J. PIETRAFESA AND GERALD S. JANOWITZ

Department of Marine Science & Engineering, North Carolina State University, Raleigh 27650

(Manuscript received 13 October 1980, in final form 6 March 1981)

ABSTRACT

A linear, two-dimensional model of a rotating, stratified fluid is constructed to investigate the circulation induced by a moving, localized line of surface stress. This model is used to analyze the effect of moving cold fronts on continental shelf circulation.

The nature of the induced circulation depends on the relative magnitude of the translation speed of the storm and the natural internal wave speed. If the surface stress moves slower than the internal wave speed, the disturbance is quasi-geostrophic and moves with the storm. If the storm moves faster than the internal wave speed, two sets of internal-inertial waves are produced. One set of waves is forced by the surface forcing and travels at the speed of the storm. Another set of waves is produced by reflection of the directly forced waves from the coastal wall.

We conclude that free surface deflection (slope) is responsible for the low-frequency, quasi-geostrophic currents due to passing cold fronts. The internal response is composed of free inertia waves which radiate away from the coast, leaving no residual circulation.

Model results are compared to current meter data collected during the passage of a cold front over the South Atlantic Bight on 9 January 1978. The inertia frequency response observed at the mooring is reproduced by the model calculation.

1. Introduction

Strong, rapidly moving cold fronts are common on the east coast of the United States during the winter. These cold fronts represent bands of strong winds which, for the most part, are aligned with the South Atlantic Bight (Cape Hatteras, North Carolina, to Jacksonville, Florida) coastline and move from land out to sea. As an example, consider successive positions of a cold front on 9 January 1978 (Fig. 1). This case is one of several which occurred about every ten days during January and February, 1978. Current measurements corresponding to this time are available from a mooring that was located 75 km east of Charleston, South Carolina, from 4 November 1977 to 22 January 1978. Current meter data (Fig. 2) show strong currents in response to the passage of this cold front. This paper addresses some aspects of this response.

Studies by Longuet-Higgins (1965), Lighthill (1967) and Ichiye (1976) consider the effect of moving surface forcing on an unbounded β-plane ocean. These analyses are concerned mainly with the quasi-geostrophic (Rossby wave), far-field wave structure. Kuo and Ichiye (1977) add the influence of a coastal boundary, but obtain only the quasi-geostrophic response because they use a coarse spacial grid in their numerical integration. The presence of the boundary changes markedly the solution from the unbounded case, i.e., shorter wavelength, coastally trapped waves appear.

This paper focuses on the influence of a coastal wall on the circulation produced by a moving surface stress. We construct a model to obtain the response of a rotating, linearly stratified fluid, bounded by a coastal wall, to a moving line of surface wind stress. Our model is analogous to a coastal region forced by a passing cold front.

The nature of the internal wave response is determined by the ratio of the storm translation speed to the natural internal wave speed. A wavelike internal-inertial wake is produced if the storm moves faster than the internal wave speed; otherwise, the disturbance is quasi-geostrophic and moves with the storm. For typical South Atlantic Bight conditions, the baroclinic currents produced by the storm are always wavelike.

Winds from a particular cold front passage on 9 January 1978 are used to force the model. The simulated currents compare favorably with the inertia frequency currents observed at the mooring.

In Section 2 we formulate the mathematical model which is solved by a Green's function technique. A typical model solution is displayed in Section 3. Details of the wind and current data for the 9 January 1978, cold front are given in Section 4. This section includes a comparison of the model results with the

[1] Present affiliation: Mesoscale Air-Sea Interaction Group, Meteorology Annex, Florida State University, Tallahassee 32306.

0022-3670/81/060836-13$07.25

current meter data. Section 5 contains the conclusions of the study.

2. Model formulation

An idealized model is constructed to investigate the short time scale internal response of a rotating, stratified fluid to a moving surface wind pattern. The wind pattern is chosen to be a line of stress, parallel to a straight coastline, which moves offshore at a constant speed. This wind pattern is analogous to a moving cold front. All dependent variables are invariant in the alongshore direction.

The model represents a simplified version of actual conditions. In general, neither the coastline nor the cold front are straight nor are they parallel. Any alongshore variations in the wind or coastline give rise to coastally trapped motions, e.g., Kelvin and Poincaré waves. This model is valid where the scales of alongshore variation are much larger than the length scale of the internal motion, i.e., the internal deformation radius.

The model dynamics are linearized, Boussinesq, and on an f-plane. By the assumption of alongshore invarience, the motion is confined to vertical planes. The basic state of the system is motionless and hydrostatic with a linear density profile.

The fluid motion is assumed to be inviscid except in a thin surface Ekman layer. The surface layer responds to the wind stress and forces the interior through an induced vertical velocity.

The influence of viscosity in the interior is indicated by the viscous length scale $(A/f)^{1/2}$. The vertical viscous length scale is ~3 m ($A = 10$ cm^2 s^{-1}). Only the higher internal modes ($n > 10$) have vertical variations approaching this scale. As we shall see later in this section, these higher modes move quite slowly and should not be important over much of the region of interest. The horizontal viscous length scale is ~1 km ($A = 10^6$ cm^2 s^{-1}). Again, only the unimportant higher modes have horizontal variations on this scale.

The bottom Ekman layer will certainly play a role in the dynamics. However, the spinup time for this layer is $f^{-1}E^{-1/2}$, where E $(=2A/fh^2)$ is the Ekman number. For $A = 10$ cm^2 s^{-1} and $h = 100$ km, the spinup time is 55 h. If simulations are no longer than two days, neglect of the bottom viscous layer will not introduce grave errors.

The equations governing the interior circulation are

$$\left.\begin{aligned} u_{t'} - fv &= -\rho_0^{-1}P_{x'} \\ v_{t'} + fu &= 0 \\ 0 &= -P_{z'} - g\rho \\ \rho_{t'} + w\bar{\rho}_{z'} &= 0 \\ u_{x'} + w_{z'} &= 0 \end{aligned}\right\}, \qquad (1)$$

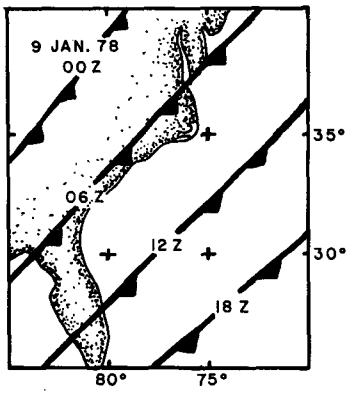

FIG. 1. Cold front location at 6 h intervals during 9 January 1978. The round symbol marks the mooring location.

where z' is positive upward, x' is positive offshore and y' is alongshore forming a right-hand triad. The velocities (u, v, w) are in the (x', y', z') directions, respectively. The mean density field is $\bar{\rho}(z)$ and ρ is a small departure from $\bar{\rho}$. P is the pressure perturbation from the hydrostatic pressure based on $\bar{\rho}$.

The coast is a straight vertical wall at $x' = 0$; the bottom is flat with a constant depth h. Surface gravity waves are eliminated by a rigid upper surface.

For the model results to apply to a variety of situations, the governing equation is solved by a Green's function technique: the wind stress has the form $(\tau^x, \tau^y) = (T^x, T^y)\delta(x' + x_0' - u_s t)$, where $\delta(x)$ is a Dirac delta function. The stress pulse moves offshore at a constant speed u_s from an initial position $x' = -x_0'$, which is over land at $t = 0$. The circulation for a given storm is obtained by combining Green's functions for several wind pulses with different initial positions.

A streamfunction is defined such that $u = -\psi_{z'}$ and $w = \psi_{x'}$. The system of equation (1) reduces to

$$\psi_{z'z't't'} + f^2\psi_{z'z'} + N^2\psi_{x'x'} = 0, \qquad (2)$$

where $N^2 = -g\rho_0^{-1}d\bar{\rho}/dz$, which is a constant. The boundary conditions are $\psi\,(x' = 0) = \psi\,(z' = -h) = 0$, which imply no normal velocity at the coastal wall and at the bottom, and $\psi\,(z' = 0) = U(x', t')$, where U is the x' transport of the Ekman layer. This last condition comes from matching the Ekman suction with the interior vertical velocity at the surface.

The independent variables are nondimensionalized such that

$$x = f(Nh)^{-1}x', \quad z = h^{-1}z', \quad t = ft'.$$

A moving variable η is introduced, where

$$\eta = (x' + x_0' - u_s t')fu_s^{-1}.$$

This variable is a position variable in the coordinate system moving with the storm. The location $\eta = 0$ is the position of the storm; $\eta > 0$ is behind the storm.

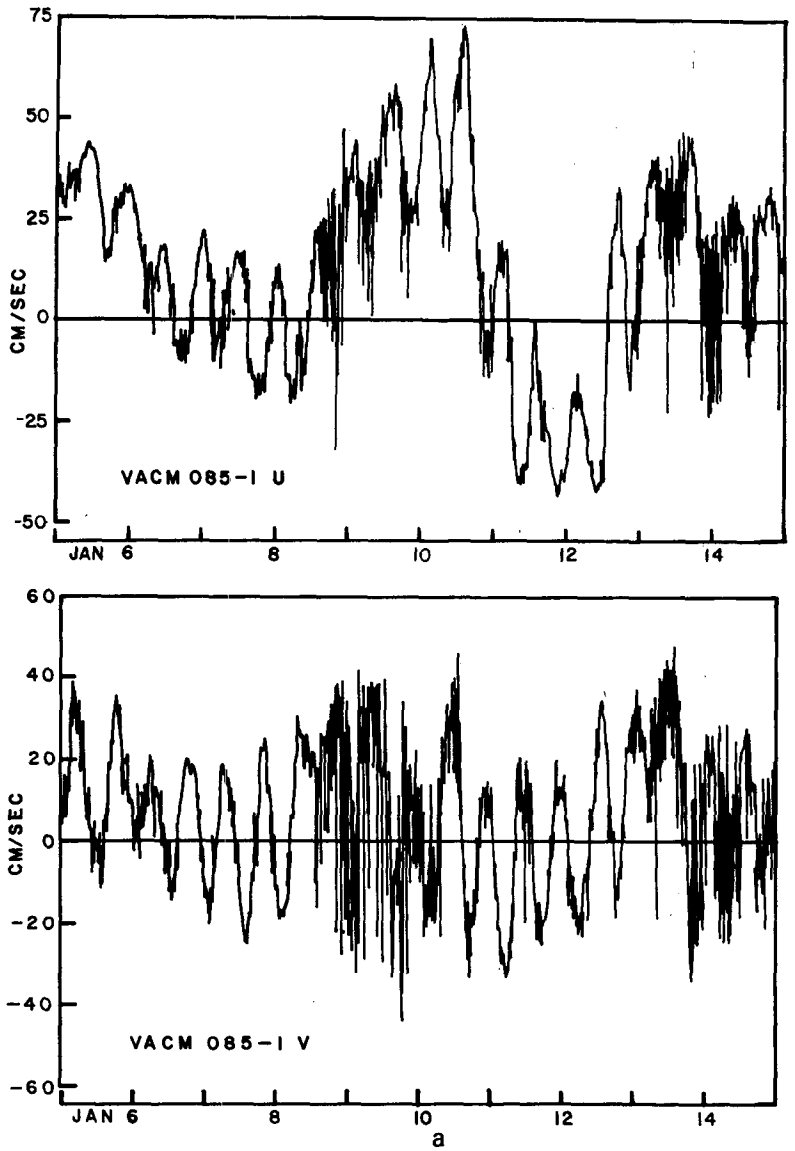

FIG. 2. Components of the raw current meter record for 5–15 January. The meter depths are (a) 10 m, (b) 22 m and (c) 42 m. Total depth is 45 m.

The interior solution is written as the sum of three terms

$$\psi(x, z, t) = (1 + z)U(\eta) + \sum_{n=1}^{\infty} A_n(\eta) \sin n\pi z + \bar{\psi}(x, z, t), \quad (3)$$

where the first term satisfies the surface boundary condition, the second is the remainder of the solution that is strictly a function of the moving variable and the last term is a homogeneous solution of (2) that cancels the first two terms at $x = 0$.

The assumed form of (3) has the following interpretation. The first two terms represent the circulation in an unbounded fluid induced by the surface forcing. With no lateral boundaries, it is natural to work in the coordinate system moving with the forcing. Lighthill (1967) makes extensive use of this idea. In such a situation, only the forced solution appears. The last term in (3) represents the effect of the lateral boundary. It is the homogeneous solution (free waves) needed to cancel the forced solution at the vertical barrier.

In terms of the moving variable, (2) becomes

$$\psi_{zz\eta} + \psi_{zz} + F^{-2}\psi_{\eta\eta} = 0, \quad (4)$$

where $F = u_s/Nh$.

Eq. (4) is the governing equation for the wake of a moving storm in a medium without lateral boundaries. The parameter F is a ratio of length scales

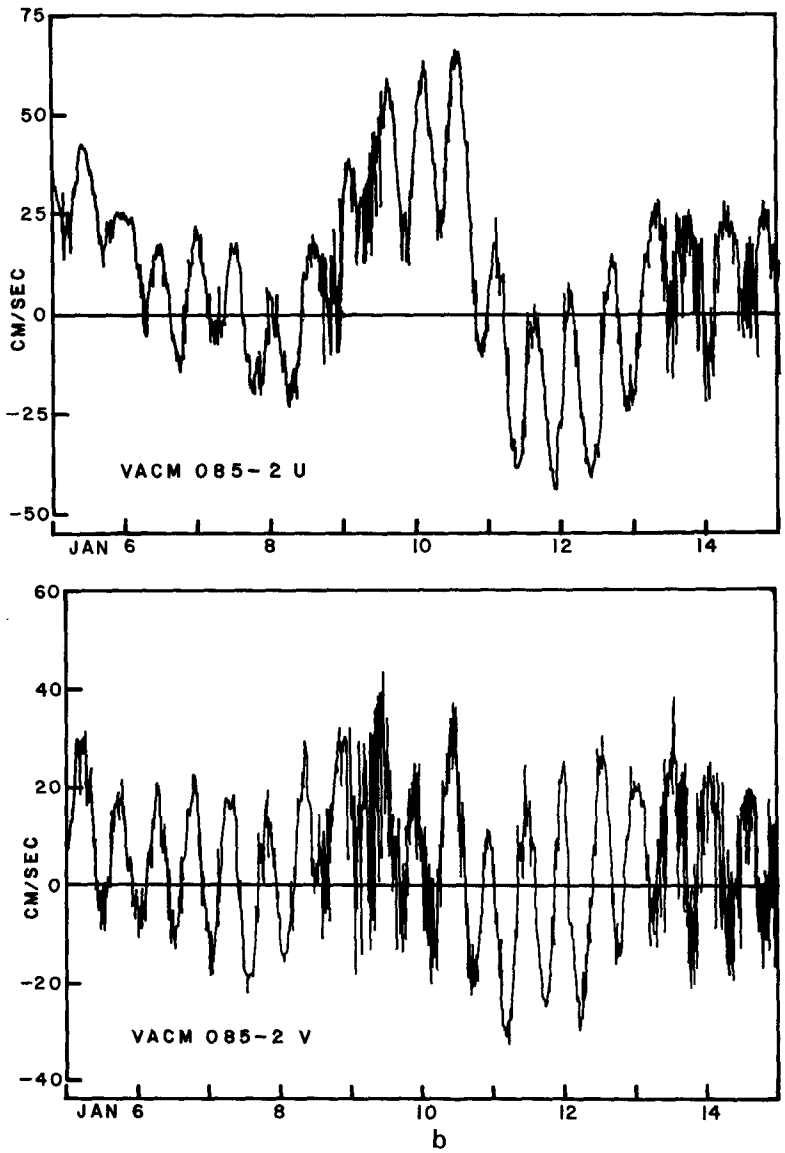

FIG. 2. (*Continued*)

L_s/L_R, where $L_s = u_s/f$ is a horizontal length scale associated with the Ekman suction induced by the moving storm and $L_R = Nh/f$ is the Rossby deformation radius, which is a horizontal length scale associated with baroclinic, geostrophic flow.

As u_s increases, the importance of the last term in (4) decreases, leaving a balance of the Coriolis and tendency terms. Therefore, rapidly moving storms leave inertia-internal waves rather than quasi-geostrophic currents.

On the other hand, as u_s decreases so that $F \ll 1$, the balance in (4) is between the second and third terms, which is the thermal wind balance. Therefore, slow storms produce quasi-geostrophic internal currents.

An equation for $A_n(\eta)$ is obtained by putting the assumed solution (3) into (4) and expanding $(1 + z)$ in the terms of the vertical modal functions, $\sin(n\pi z)$. Thus,

$$\frac{d^2}{d\eta^2} A_n + \gamma_n^2 A_n = -2\gamma_n^2 (n\pi)^{-3} F^{-2} \frac{d^2}{d\eta^2} U, \quad (5)$$

where $\gamma_n^2 = (n\pi F)^2[(n\pi F)^2 - 1)]^{-1}$. The forcing term in (5) is the horizontal variation of the Ekman suction due to the surface stress.

The solution to (5) depends on the sign of γ_n^2. If $F > (n\pi)^{-1}$, then $\gamma_n^2 > 0$ and the homogeneous solutions are trigonometric. This situation corresponds to a rapidly moving storm which produces inertial oscillations. The dimensional condition for a wavelike wake is $u_s > Nh(n\pi)^{-1}$. Therefore, if

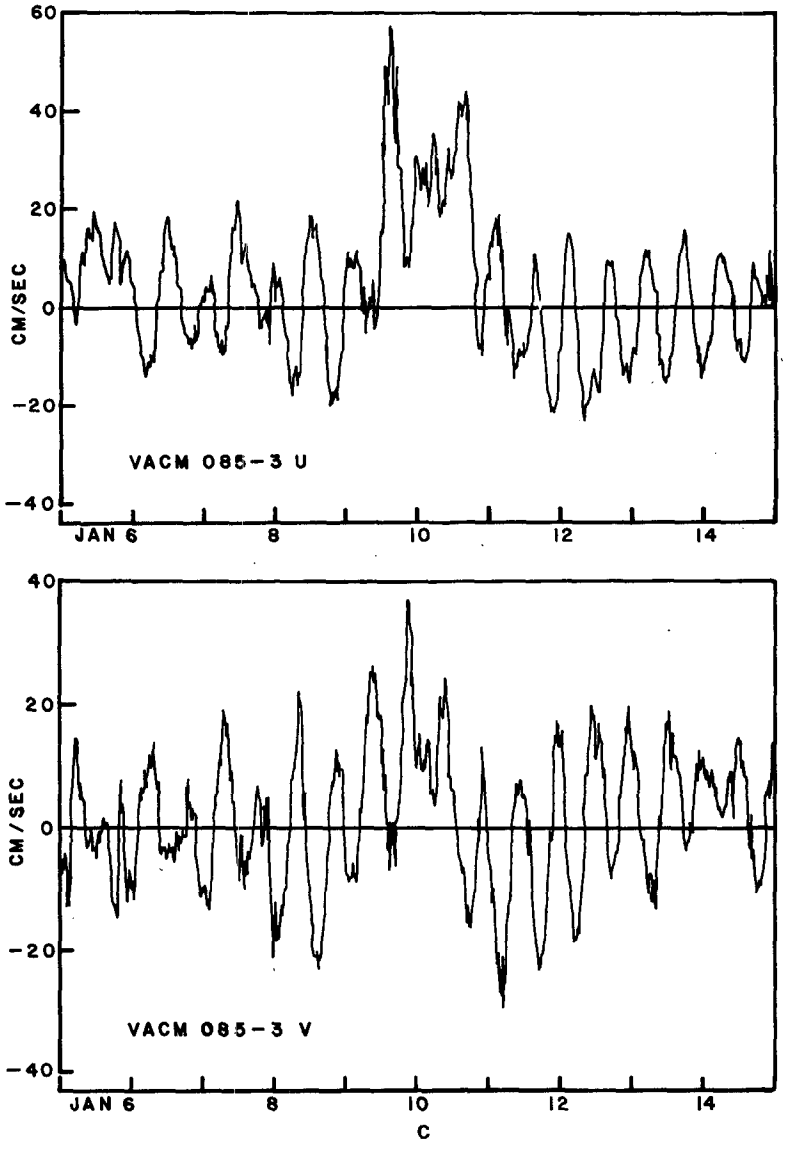

FIG. 2. (*Continued*)

the surface forcing moves faster than the internal wave speed, an inertial wave wake is produced.

If $\gamma_n^2 < 0$, the solutions to (5) are exponential. In this case, the directly forced disturbance is bound to the storm. As the storm moves slower, the disturbance becomes more geostrophic. The limiting case is obtained when the storm no longer moves and the response is steady, wind-forced geostrophic flow.

If $F = (n\pi)^{-1}$ for any n, (5) becomes singular indicating a resonant response of the water to the surface stress. As the storm speed decreases, the $n = 1$ mode will resonate before the higher modes.

The expected oceanic response to moving cold fronts in the South Atlantic Bight is determined from the condition $u_s > Nh(n\pi)^{-1}$. If $h = 50$ m and $N = 10^{-1}$ s^{-1} (highly stratified) then storms must move faster than ~ 2 m s^{-1} for a wavelike internal response. Atmospheric systems generally pass over the South Atlantic Bight at ~ 5 m s^{-1} (Pietrafesa *et al.*, 1978). Therefore, the typical internal response to moving systems is wavelike. For the remainder of the paper, γ_n^2 is taken to be positive.

Eq. (5) can be solved without knowing $U(\eta)$ by invoking the method of variation of constants (Butkov, 1968). The solution is

$$A_n(\eta) = 2\gamma_n(n\pi)^{-3}F^{-2}\left[-\sin(\gamma_n\eta)\int_0^\eta \cos(\gamma_n\eta')U''(\eta')d\eta' + \cos(\gamma_n\eta)\int_0^\eta \sin(\gamma_n\eta')U''(\eta')d\eta'\right],$$

where U'' is the second derivative of $U(\eta)$ with respect to η. This expression is valid for $\eta > 0$ which corresponds to positions behind the storm. Because the storm moves faster than the internal waves, there is no disturbance ahead of the forcing.

The homogeneous internal solution [third term in (3)] satisfies (2) which in terms of the nondimensional variables is

$$\bar{\psi}_{zztt} + \bar{\psi}_{zz} + \bar{\psi}_{xx} = 0. \tag{6}$$

The boundary condition on $\bar{\psi}$ at the wall requires the sum of the first two terms of (3) at $x = 0$. It has the general form

$$\psi\,(x = 0) = \sum_{n=1}^{\infty} g_n(t)\,\sin(n\pi z),$$

where $g_n(t) = A_n(t - x_0/F) - 2(n\pi)^{-1}U(t - x_0/F)$. For the total streamfunction to vanish at the coastal wall, the boundary condition on $\bar{\psi}$ must be

$$\bar{\psi}\,(x = 0) = -\sum_{n=1}^{\infty} g_n(t)\,\sin(n\pi z).$$

The boundary conditions in the vertical are $\bar{\psi}(z = 0) = \bar{\psi}(z = -1) = 0$. To avoid energy at infinity, the solution also must be bounded as $x \to \infty$.

Given the boundary conditions, the solution of (6) is found in terms of vertical modes,

$$\bar{\psi}(x, z, t) = \sum_{n=1}^{\infty} \phi_n\,\sin(n\pi z).$$

The governing equation for ϕ_n is obtained from (6) as

$$(\phi_n)_{tt} + \phi_n - (n\pi)^{-2}(\phi_n)_{xx} = 0, \tag{7}$$

with boundary conditions $\phi_n(x = 0) = -g_n(t)$, $\phi_n(t < x_0/F) = 0$ and $\phi_n(x \to \infty) \to 0$.

Eq. (7) has the form of a rotationally modified wave equation for the amplitude of each vertical mode. The nondimensional phase speed is $\pm(n\pi)^{-1}$; the higher modes have a slower propagation speed. Each mode is forced by a time dependent amplitude $g_n(t)$ at the coastal wall which is the reflection of the directly forced internal waves from the coastal wall.

The mathematical problem in (7) is solved by a Laplace transform in t since ϕ_n vanishes for $t < 0$. The transform of (7) is

$$\frac{d^2}{dx^2}\bar{\phi}_n - (n\pi)^2(s^2 + 1)\bar{\phi}_n = 0,$$

where the overbars denote the Laplace transform of the indicated variable. The boundary conditions are $\bar{\phi}_n\,(x = 0) = -\bar{g}_n$ and $\bar{\phi}_n\,(x \to \infty) \to 0$.

The solution for $\bar{\phi}_n$, obeying the boundary conditions, is

$$\bar{\phi}_n = -\bar{g}_n\,\exp[-n\pi x(s^2 + 1)^{1/2}].$$

The inverse transform of the exponential term is obtained from Erdelyi (1954, p. 248, rule 23). The solution to (7) is

$$\phi_n(x, t) = -g_n(t) * [\delta(t - n\pi x - x_0/F) - n\pi x y^{-1} J_1(y)], \tag{8}$$

where $y^2 = (t - x_0/F)^2 - (n\pi x)^2$, an asterisk denotes the process of convolution and J_1 is the first-order Bessel function of the first kind.

The nature of the solution in (8) is seen most easily by letting $g_n(t)$ be a delta function, which will give a single impulsively started wavetrain. For this choice of $g_n(t)$, (8) becomes

$$\phi_n(x, t) = S(t - n\pi x - x_0/F) \times [1 - n\pi x J_1(y) y^{-1}],$$

where $y^2 = (t - x_0/F)^2 - (n\pi x)^2$ and $S(x)$ is the Heaviside unit step function. This impulsive solution has the form of a wave front propagating at the internal wave speed $(n\pi)^{-1}$ and trailing inertia-internal waves. For large time at any x ($t \gg n\pi x$), y becomes large and

$$y^{-1}J_1(y) \sim (2/\pi t^3)^{1/2}\cos(t - \tfrac{3}{4}\pi).$$

The amplitude of the internal waves decays at $t^{-3/2}$ for large times. This dissipation occurs, not by viscous forces, but by energy being spread by the wave field over a larger area. This result is similar to that obtained by Cahn (1945) in which inertia waves radiate from the region of an impulsively started current. A further discussion of impulsively started internal waves appears in McNider and O'Brien (1973).

The solution in (8), therefore, is a series of inertia-internal waves created by the reflection from the coastal wall of the directly forced internal waves.

The explicit solution to the moving storm problem is found by choosing the Ekman layer dynamics. Various models for the Ekman layer can be considered at this point; however, the usual equations for the vertically integrated transport in the Ekman layer, neglecting external pressure gradients, are

$$\left.\begin{aligned} U_t - V &= T^x f^{-1}\delta(\eta) \\ V_t + U &= T^y f^{-1}\delta(\eta) \end{aligned}\right\}. \tag{9}$$

It is assumed that the Ekman layer is thin enough for the density variations within the layer to be unimportant. If the transport vanishes before the pulse ($\eta < 0$), then the solution for $U(\eta)$ is

$$U(\eta) = T^x\cos\eta + T^y\sin\eta. \tag{10}$$

Now that U is known, it is straightforward to generate $A_n(\eta)$, $g_n(t)$ and $\phi_n(x, t)$ as outlined above. The total streamfunction is

$$\psi(x, z, t) = S(\eta)\sum_{n=1}^{\infty}[-2(n\pi)^{-1}(T^x\cos\gamma_n\eta + T^y\gamma_n^{-1}\sin\gamma_n\eta) + 2(n\pi f)^{-1}\phi_n(x, t)]\sin(n\pi z), \tag{11}$$

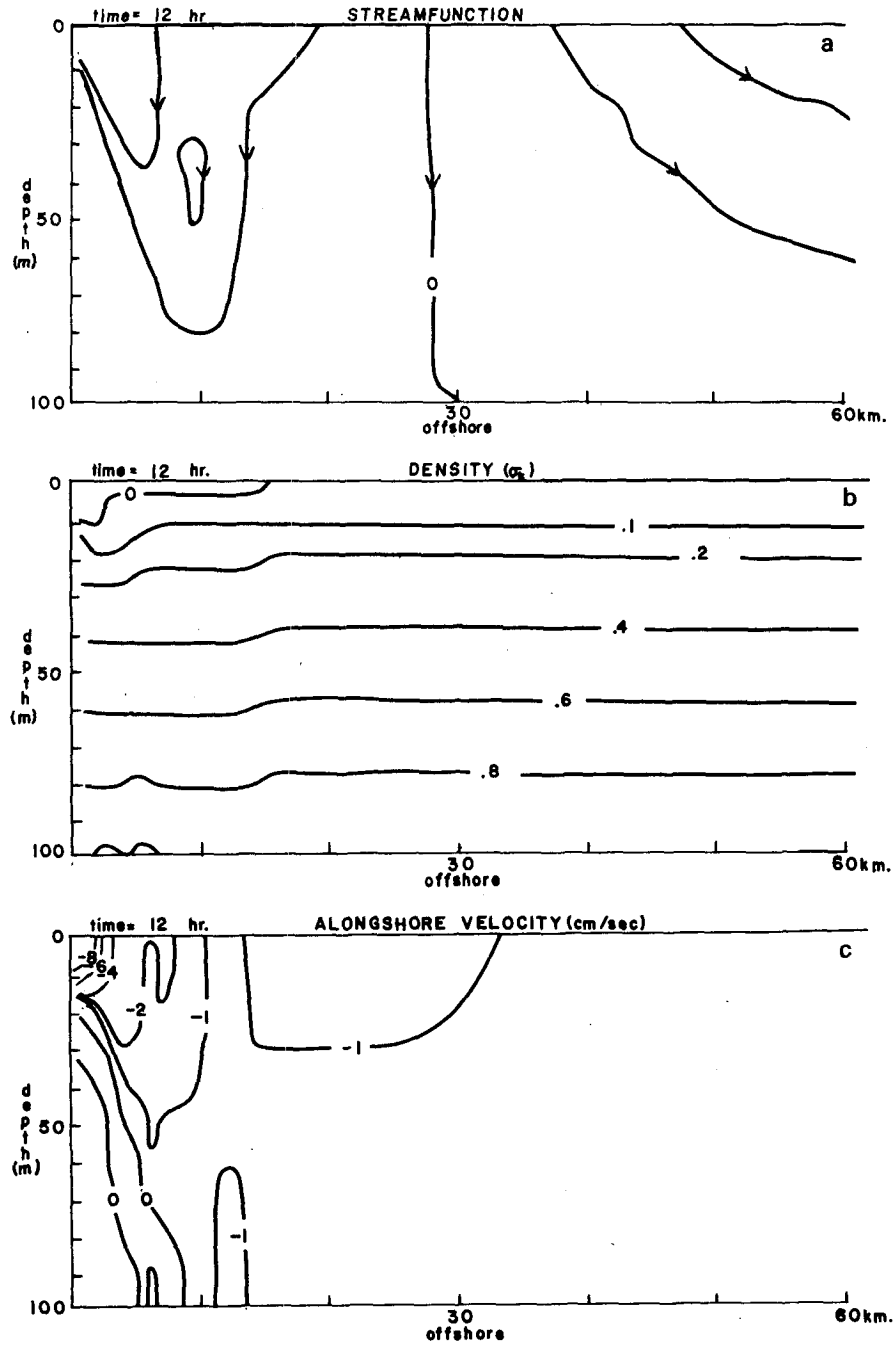

FIG. 3. Green's function solution at $t = 12$ h for a single alongshore wind pulse. The streamfunction is nondimensionalized by τ/f and the contour interval is 0.2. The density is the sum of the linear base state and the perturbation. The alongshore velocity is in cm s^{-1}.

where

$$\phi_n(x, t) = S(\lambda_n)\Big\{-T^x \cos\gamma_n\lambda_n - T^y\gamma_n^{-1}\sin\gamma_n\lambda_n + 2x\int_{n\pi x + x_0/F}^{t} [T^x \cos\gamma_n(t - t') + T^y\gamma_n^{-1}\sin\gamma_n(t - t')]J_1(y)y^{-1}dt'\Big\},$$

$$y^2 = (t' - x_0/F)^2 - (n\pi x)^2,$$

$$\lambda_n = (t - n\pi x - x_0/F),$$

and $S(x)$ is the Heaviside unit stepfunction.

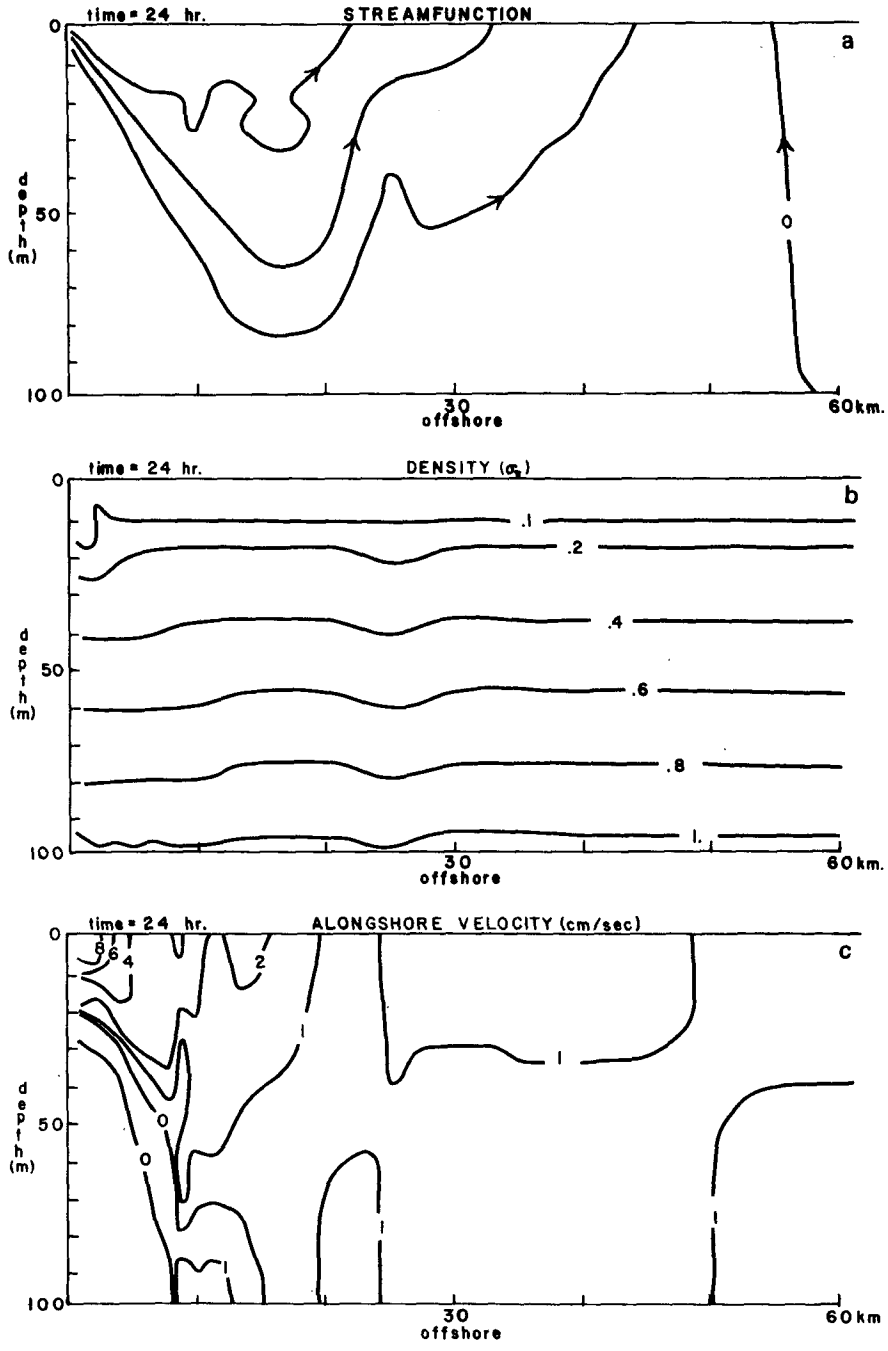

FIG. 4. Green's function solution at t = 24 h. See explanation in Fig. 3.

The three velocity components and density perturbation can be obtained from this formula. The expressions are quite lengthy and are not listed here. They are given in Klinck (1980).

3. Discussion

This model of circulation induced by a moving storm is appropriate for winter conditions in the South Atlantic Bight. Strong, frequent storms keep the shelf waters well mixed, though there is usually a small density difference ($<1\sigma_t$) over the whole water column. During the summer, a strong thermocline develops making a two-layer model more appropriate.

The Green's function solution is displayed for typical South Atlantic Bight conditions. The parameters are $f = 10^{-4}$ s^{-1}, $h = 100$ m, $N = 10^{-2}$ s^{-1} and

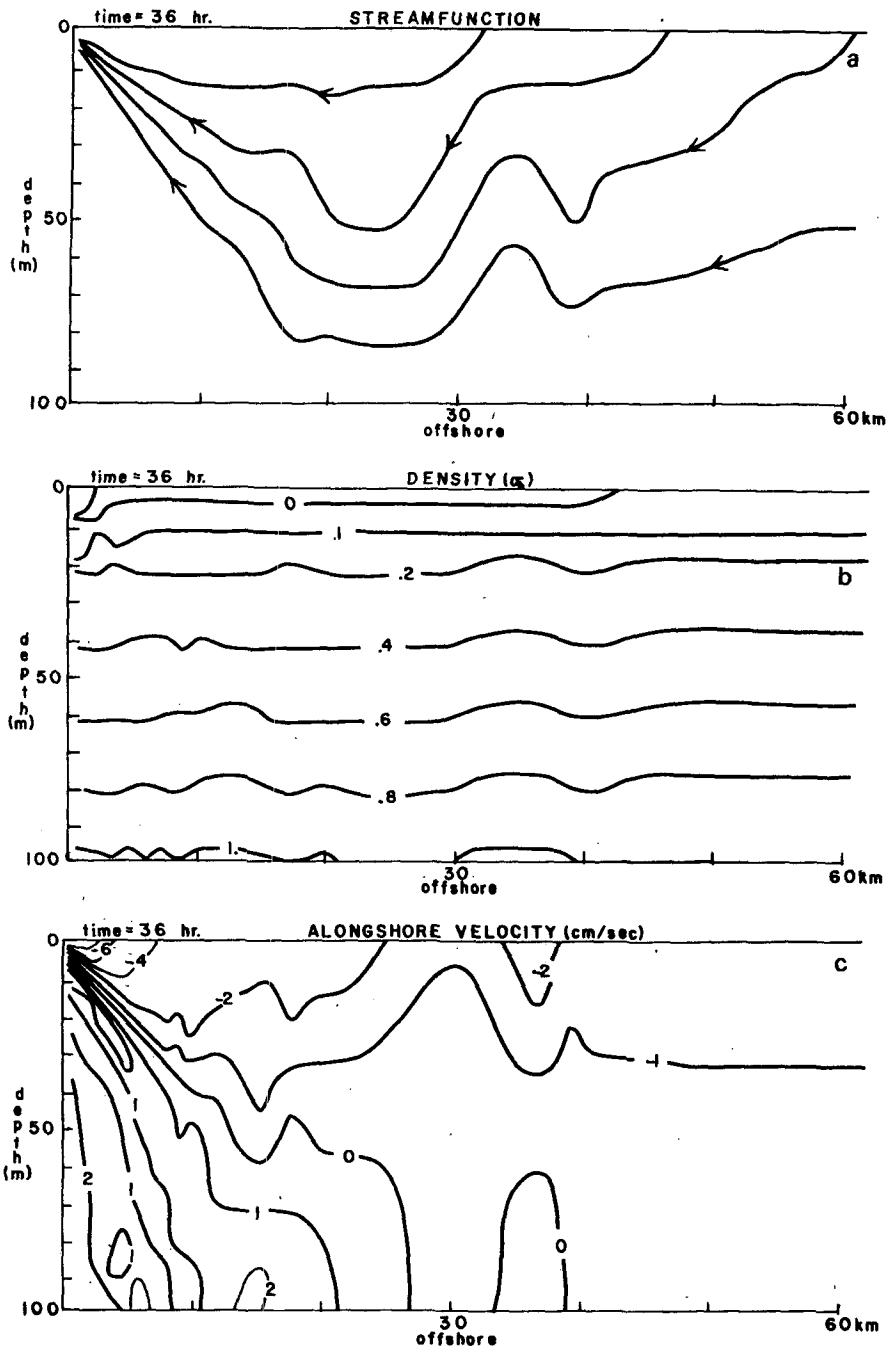

FIG. 5. Green's function solution at $t = 36$ h. See explanation in Fig. 3.

$u_s = 5$ m s^{-1}. The wind is an alongshore wind pulse with a magnitude of 1 dyn cm^{-2}.

The convolution integral in (11) is calculated numerically with a 20 node Gaussian integration scheme, which was tested against higher numbers of nodes and was found to be in excellent agreement. The numerical sums were carried out to 60 terms; convergence of the series was slow in some places, especially near the coast.

The Green's function solution at twelve hour intervals is shown in Fig. 3, 4 and 5. Note that only the interior solution is displayed; the Ekman layer is ignored in these figures. The single wind pulse arrives at the coast at $t = 0$. After 12 h (Fig. 3), the pulse is 72 km offshore, just beyond the right edge of the graph. Most of the circulation is the directly forced part of the solution, represented by broad features with low velocities. The strong disturbance

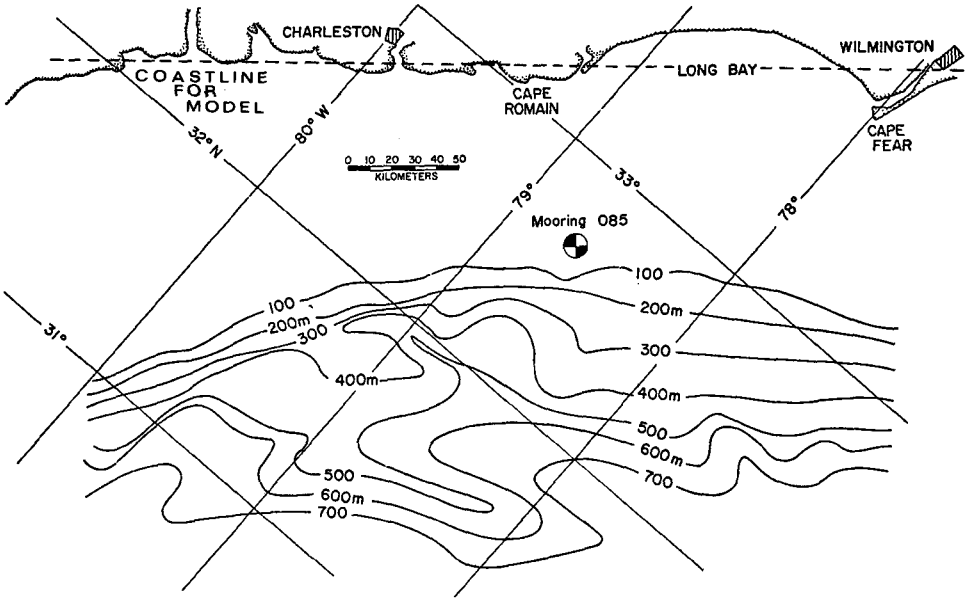

FIG. 6. Mooring location and coastal topography near Charleston, South Carolina. The dashed line indicates the position of the assumed vertical coastal wall.

10 km from the wall is the $n = 1$ mode wave reflected from the coastal wall. The length scale associated with this wave is the Rossby radius Nh/f, which in this calculation is 11 km.

The density field is mainly a superposition of the large scale directly forced wave and the first mode wall reflected wave. During this phase of the directly forced wave, the vertical velocity is downward, producing a large scale lowering of the density field. The wall-reflected wave further lowers the density field near the wall.

The strongest alongshore velocities are associated with the reflected wave near the wall. The large velocities near the wall are created by the superposition of higher mode, slower moving waves.

After 24 and 36 h (Fig. 4 and 5), more details of the wave field are visible. The directly forced wave remains clearly visible as the broad scale currents reverse direction between figures. The inertia period for this simulation is about 21 h. The large-scale density field is clearly moving up and down between figures in response to the direct forcing. Away from the coastal wall, the alongshore velocity reverses inertially.

The wave front associated with the $n = 1$ wall reflected wave remains clearly visible in the solution. There is an indication in Fig. 5 at 15 km of an $n = 2$ mode reflected wave. This wave is somewhat obscured by the continued production of $n = 1$ waves as the Ekman layer reverses. The single storm pulse starts the Ekman layer which continues to oscillate in the absence of frictional dissipation.

This "ringing" of the Ekman layer continuously forces the interior flow producing a continuing train of directly forced and wall reflected waves. This unrealistic feature of the Green's function solution is a result of the impulsive character of the surface wind forcing. In a general simulation of an extended wind system, the surface layer starts and stops as the stress direction and magnitude changes. Thus, ringing of the Ekman layer is not a problem when the Green's function solutions are combined to simulate the induced circulation due to an extended wind system such as a cold front.

The internal response due to the wind structure of a cold front is obtained by superposing Green's functions for a series of wind pulses with different initial positions (x_0'). The Green's function is combined by integrating the solution (11) over x_0 with T^x and T^y replaced by appropriate functions of x_0. Since the convolution integral is calculated numerically, excessive computer time would be required to evaluate the required iterated integral. Instead, the Green's function is evaluated approximately as

$$\psi(x, z, t) = \int_0^\infty \psi_G(x, z, t: x_0)dx_0 \approx \sum_{n=1}^{N} \psi_G(x, z, t: x_n) + E_N, \quad (12)$$

where ψ_G is the Green's function given in (11) and depends implicitly on the forcing. In the discrete form, x_n corresponds to the initial positions of the pulses that make up the extended storm. Error analysis (Klinck, 1980) shows that an upper bound to the relative error, $E_N f/\tau$, in (12) is $fX[2u_s(N-1)]^{-1}$, where X is the total horizontal extent of the storm.

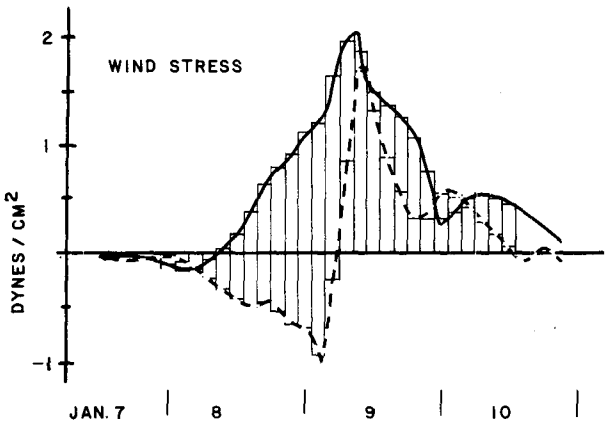

FIG. 7. Wind stress components calculated from National Weather Service observations at Charleston, South Carolina. The dashed line is the across-shore stress; the solid line is the alongshore stress. The boxes show the magnitude of the 26 pulses used to simulate the cold front passage.

For a given simulation and choice of maximum error, this expression indicates the number of pulses to use.

The model is tested for one case of a cold front passage over Charleston, South Carolina, on 9 January 1978 for which current measurements are available.

4. Comparison with data

A current meter mooring off Charleston provided a good data set for comparison with model results. The mooring was located on the 45 m isobath at 33°38'N, 78°42'W (Fig. 6) from 4 November 1977 to 22 January 1978. Three vector-averaging current meters (VACM) were attached to the mooring cable at depths of 10, 22 and 42 m.

A strong cold front, parallel to the coast passed over the mooring on 9 January 1978. Successive positions of the front (Fig. 1) are taken from the National Weather Service surface barometric charts. An estimate of the translation speed of the front from these positions is 18 m s^{-1}. Wind measurements from the National Weather Service station at Charleston, S.C. (available from the National Climatic Center, Asheville, North Carolina) are used to calculate the surface wind stress. These coastal wind values are increased by 50% to account for the increased strength of offshore winds (Weisberg, personal communication). The surface wind stress is calculated by a quadratic drag law with a drag coefficient of 1.5×10^{-3} (Pond, 1975). The stress components (Fig. 7) are shown relative to the coastline orientation which at Charleston is 50° east of north.

The required number of pulses is determined by the choice of maximum allowed error. For a 10% upper bound on the error, the wind must be averaged over 40 min, requiring 55 pulses for the entire event. The Coriolis parameter appropriate for Charleston is 0.8×10^{-4} s^{-1}. If a 30% relative error is allowed, the stress is averaged over 0.1 day and 26 pulses are required. This second choice is made to reduce computer costs.

Frequent, intense winter storms keep shelf waters off Charleston well mixed. However, the current meters indicate a temperature difference of 1°C between the top and bottom meters. Assuming a weak salinity influence on the density, this temperature differential implies a density difference of $0.3\sigma_t$ in 32 m resulting in a Brünt-Väisälä frequency of 10^{-2} s^{-1}. The nature of the internal response is determined from these parameters by evaluating $F = u_s/Nh$, which in this case $F = 40$. Since $F > \pi^{-1}$, the internal circulation is wavelike.

The current meter data contain three types of motion not included in the model: tides, low frequency, quasi-geostrophic currents and currents due to surface gravity waves. The semi-diurnal tides are

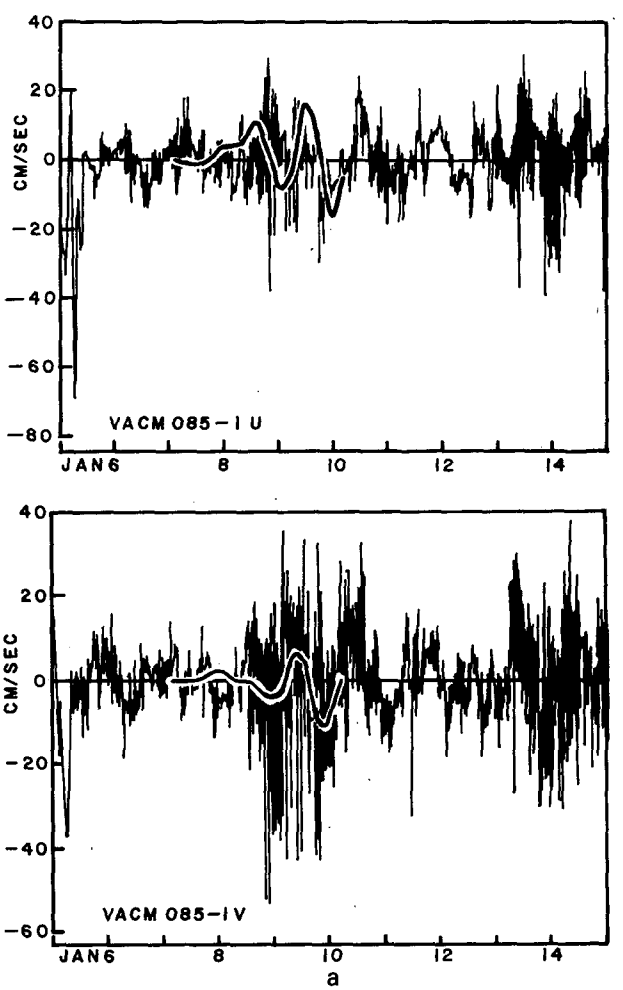

FIG. 8. Comparison of the model simulation with the modified current meter record. The 40 h low-pass series and the 12.4 h tide records are subtracted from the raw record. The solid, overlaid line is the corresponding model result.

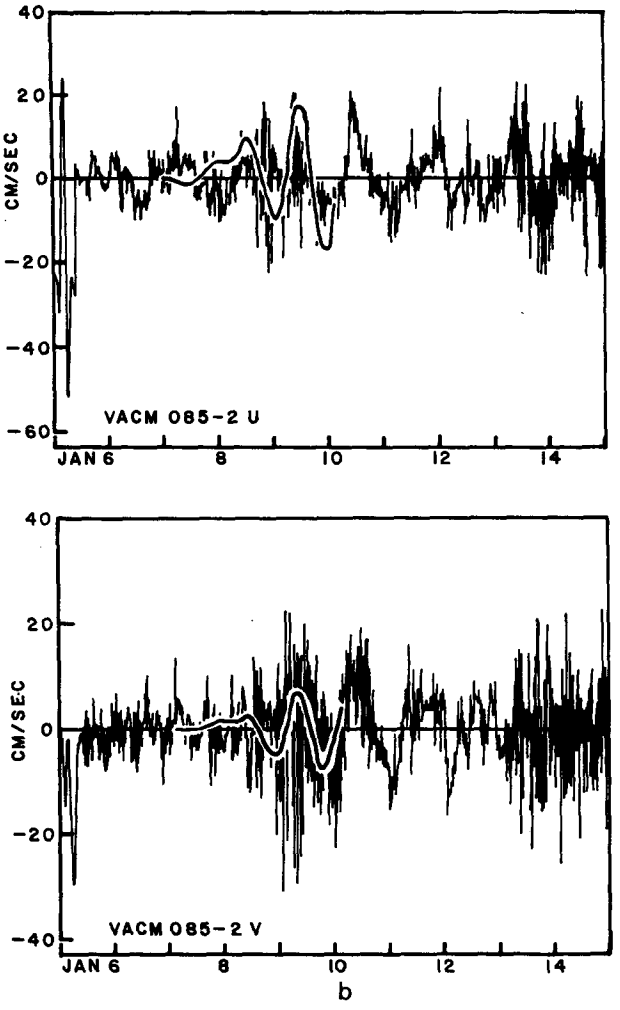

FIG. 8. (*Continued*)

prominent in all raw current records (Fig. 2). This signal is removed by band-pass filtering the raw record at 12.4 h to obtain the tidal signal, which is subtracted from the raw data.

The low frequency, quasi-geostrophic signal is removed by a similar process. These currents are nearly barotropic due to large-scale changes in sea surface elevation. The raw data is low-pass filtered with a half-power point at 40 h. This low-frequency signal is subtracted from the series with the tides removed to obtain the inertial and higher frequency currents (Fig. 8) for 10 days spanning the passage of the front.

For the time span considered, only the directly forced part of the solution is important. The fastest wall reflected mode has a translation speed of 12 cm s^{-1}. At this rate, 7.3 days are required for the wall reflected wave to reach the mooring.

Fig. 8 shows the u (east) and v (north) components of the modified current observations during the passage of the front. The solid, overlaid lines are the corresponding model results in this coordinate system.

The top meter shows considerable high-frequency motion due to surface waves. Maxima and minima of the model results match the corresponding peaks in the current meter data. The middle meter (Fig. 8b), being deeper, has less high-frequency noise than the top meter. The model results compare well in amplitude and phase with the measured currents. The bottom meter (Fig. 8c) shows the cleanest comparison between measurements and the model. By the middle of 8 January the model results compare well to the measured currents. Model results lead the current meter somewhat because friction retards the measured current but not the model currents. The overall comparison of measurements and the model is quite good.

Model results stop after 10 January for several reasons. Mainly, the model is not valid after two days or so because of the neglect of the bottom Ekman layer. Also, the major effects of the storm

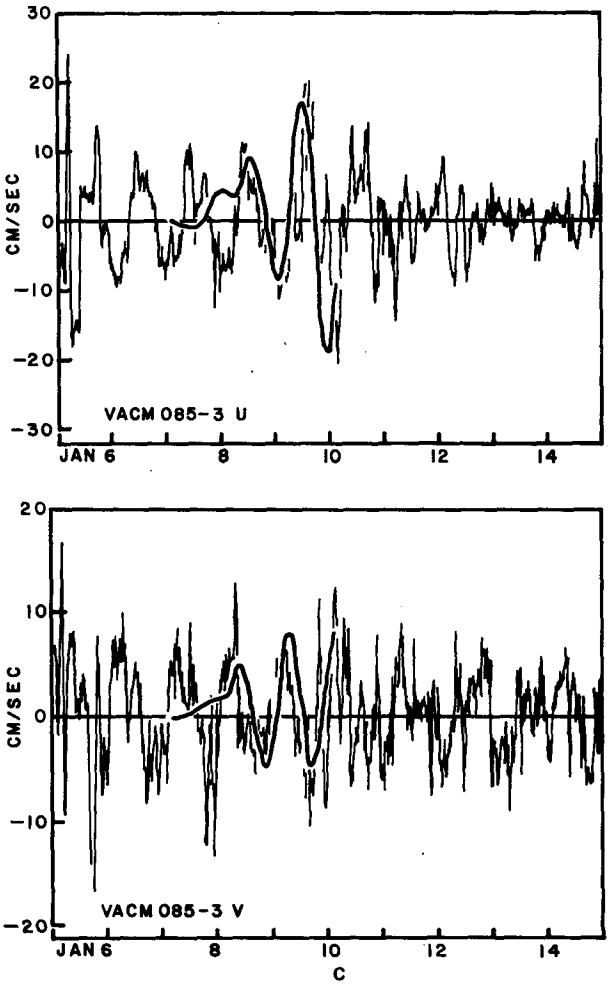

FIG. 8. (*Continued*)

have passed and the currents are beginning to subside. The model is not valid for decay of the currents after storm passage because the interior viscous effects are neglected. Most importantly, the surface Ekman layer continues to oscillate in the absence of dissipation; thus, continually forcing the interior circulation. A model with a more robust description of viscous effects is required to handle the spin-down stage after the storm has passed.

5. Conclusions

A linear model of a rotating, linearly stratified fluid is constructed to investigate the response of a flat-bottom coastal area to a moving surface wind stress. This model is used to analyze the effects of moving cold fronts on a continental shelf, in particular the South Atlantic Bight.

The nature of the internal current induced by the moving storm depends on the relative magnitude of the storm speed and the natural internal wave speed. For a storm moving slower than the internal wave speed the disturbance is quasi-geostrophic and moves with the storm. If the storm moves faster than the internal speed, the internal response consists of two sets of inertia waves. One set of waves is directly forced by the moving surface stress and moves at the speed of the storm. The other set of waves arises from reflection of the directly forced wave from the coastal wall. These waves radiate from the wall with slowly decreasing amplitude. The frequency of the waves also decreases, tending asymptotically to the inertia frequency.

Parameters for a given cold front and coastal area can be used to predict the nature of the internal response. Two length scales are pertinent to this analysis: the length scale of the moving storm ($L_s = U_s/f$) and the internal Rossby radius ($L_R = Nh/f$), which is the length scale associated with baroclinic geostrophic currents. If $L_s/L_R > \pi^{-1}$, then the wake is wavelike; otherwise it is quasi-geostrophic. For $\pi L_s/L_R$, the pressure gradient is too small to balance the Coriolis term, so the inertia balance remains. If $\pi L_s < L_R$, the pressure gradient is larger and the dynamic balance is quasi-geostrophic.

The cold front on 9 January 1978 did produce a low-frequency quasi-geostrophic response (Fig. 2) which is principally the result of free surface slope. If a free surface Rossby radius [$L_R' = (gh)^{1/2}/f$], is used in the above length scale analysis, we see that $L_s/L_R' < \pi^{-1}$, implying a quasi-geostrophic rather than inertia wave response. Therefore, the low-frequency currents induced by moving storm systems, for the most part, are the result of induced free surface slope, not deformations of the internal density field.

Acknowledgments. The authors wish to thank Dr. J. J. O'Brien for making valuable comments and suggestions and Eileen Hofmann for critical comments on the manuscript. This work is part of a dissertation submitted by J. Klinck to North Carolina State University in partial fulfillment of the requirements for a Ph.D. degree.

This work was supported by U.S. Department of Energy under Contract DOE-AS09-76-EY00902 and the U.S. Bureau of Land Management under Contract AA 550-CT7-29-025.

REFERENCES

Butkov, E., 1968: *Mathematical Physics*. Addison-Wesley, 735 pp.

Cahn, A., 1945: An investigation of the free oscillations of a simple current system. *J. Meteor.*, **2**, 113–119.

Erdelyi, A., Ed., 1954: *Table of Integral Transforms*, Vol. I. McGraw-Hill, 391 pp.

Ichiye, T., 1976: Barotropic disturbances caused by a point storm in a β-plane ocean—Part I, Asymptotic analysis. *J. Oceanogr. Soc. Japan*, **32**, 33–47.

Klinck, J., 1980: Continental shelf circulation induced by a moving, localized wind stress. Ph.D. dissertation, North Carolina State University, Raleigh, 131 pp.

Kuo, H. H., and T. Ichiye, 1977: A numerical study of the response of a barotropic ocean to a moving hurricane. *Tellus*, **29**, 561–571.

Lighthill, M. J., 1967: On waves generated in dispersive systems by travelling forcing effects, with applications to the dynamics of rotating fluids. *J. Fluid Mech.*, **27**, 725–752.

Longuet-Higgins, M. S., 1965: The response of a stratified ocean to stationary or moving wind-systems. *Deep Sea Res.*, **12**, 923–973.

McNider, R. T., and J. J. O'Brien, 1973: A multi-layer transient model of coastal upwelling. *J. Phys. Oceanogr.*, **3**, 258–273.

Pietrafesa, L. J., R. D'Amato, C. Gabriel and R. J. Sawyer, Jr., 1978: Continental margin atmospheric climatology and sea level 1974–75. UNC Sea Grant Publ. UNC-SG-78-09, 187 pp.

Pond, S., 1975: The exchanges of momentum, heat and moisture at the ocean-atmosphere interface. *Numerical Models of Ocean Circulation*, Nat. Acad. Sci., 26–38.